Depletion of TSG101 forms a mammalian 'Class E' compartment: a multicisternal early endosome with multiple sorting defects

Aurelie Doyotte[1,*], Matthew R. G. Russell[2,*], Colin R. Hopkins[2] and Philip G. Woodman[1,‡]

[1]Faculty of Life Sciences, University of Manchester, Manchester, M13 9PT, UK
[2]Department of Biological Sciences, Imperial College, London, SW7 2AS, UK
*These authors contributed equally to this work
‡Author for correspondence (e-mail: philip.woodman@manchester.ac.uk, c.hopkins@imperial.ac.uk)

Accepted 6 April 2005
Journal of Cell Science 118, 3003-3017 Published by The Company of Biologists 2005
doi:10.1242/jcs.02421

Summary

The early endosome comprises morphologically distinct regions specialised in sorting cargo receptors. A central question is whether receptors move through a predetermined structural pathway, or whether cargo selection contributes to the generation of endosome morphology and membrane flux. Here, we show that depletion of tumour susceptibility gene 101 impairs the selection of epidermal growth factor receptor away from recycling receptors within the limiting membrane of the early endosome. Consequently, epidermal growth factor receptor sorting to internal vesicles of the multivesicular body and cargo recycling to the cell surface or Golgi complex are inhibited. These defects are accompanied by disruption of bulk flow transport to the lysosome and profound structural rearrangement of the early endosome. The pattern of tubular and vacuolar domains is replaced by enlarged vacuoles, many of which are folded into multicisternal structures resembling the 'Class E' compartments that define several *Saccharomyces cerevisiae* vacuolar protein sorting mutants. The cisternae are interleaved by a fine matrix but lack other surface elaborations, most notably clathrin.

Key words: endocytosis, multi-vescicular body (MVB), ESCRT, GFR, transferrin

Introduction

Internalised transferrin receptors (TR) and epidermal growth factor receptors (EGFR) are delivered to the early endosome, a common compartment consisting of tubules and vacuoles (Gruenberg and Maxfield, 1995; Mellman, 1996; Trowbridge et al., 1993). Within the larger vacuoles in this compartment, the different receptor populations become separated; the EGFR become concentrated on the internal vesicles that form as the vacuole matures into a multi-vesicular body (MVB) whilst the TR remain on the perimeter membrane (Felder et al., 1990; Hopkins et al., 1990). Subsequently the EGFR are delivered to the lysosome and degraded whilst the TR are recycled (Felder et al., 1990; Hopkins et al., 1990). The sorting mechanisms responsible for separating these two sub-sets of trafficking proteins are currently being characterised in detail. Recent studies suggest that EGFR and other mitogenic receptors become concentrated in discrete domains on the MVB perimeter membrane because they are ubiquitinated (Haglund et al., 2003; Raiborg et al., 2002) and/or promote the ubiquitination of associated factors (van Delft et al., 1997; van Kerkhof et al., 2001). These domains are readily identifiable by electron microscopy because they bear a bristle coat on the cytosolic face containing clathrin heavy chain (Sachse et al., 2002). They also contain Hrs (hepatocyte growth factor receptor substrate), a cytosolic protein which is a substrate for tyrosine receptor kinases (Komada and Kitamura, 1995) and which binds to clathrin directly (Raiborg et al., 2001). Cells lacking Hrs show impaired EGFR down-regulation (Lloyd et al., 2002), and additional studies have implicated Hrs in MVB morphogenesis (Bache et al., 2003a; Komada and Soriano, 1999; Urbe et al., 2003).

The relationship between the clathrin/Hrs domains and the invagination that gives rise to the internal vesicles is not known. However, Hrs is able to bind ubiquitinated proteins such as EGFR (Bishop et al., 2002; Lloyd et al., 2002; Polo et al., 2002) and at the same time interact, via proline-rich motifs, with a protein complex termed ESCRT-I (endosomal sorting complex required for transport I) (Bache et al., 2003a; Bilodeau et al., 2003; Katzmann et al., 2003; Pornillos et al., 2003). ESCRT-I was first identified in *Saccharomyces cerevisiae*, where it mediates ubiquitin-dependent MVB sorting via the ubiquitin binding activity of one subunit, Vps23p (Katzmann et al., 2003). The mammalian orthologue of Vps23p, TSG101 (tumour susceptibility gene 101), also binds ubiquitin and is involved in EGFR sorting (Babst et al., 2000; Bishop et al., 2002; Garrus et al., 2001), though its precise function remains poorly characterised. Nevertheless, a plausible hypothesis is that ubiquitinated EGFR become concentrated in the Hrs/clathrin domain and as a result of their interaction with the ESCRT-I complex they are delivered to the internal vesicles of the MVB. TR normally remain on the perimeter membrane of the MVB, are excluded from the Hrs-

containing domain and recycle. However, when artificially ubiquitinated they associate with Hrs, do not recycle and most likely also become directed to the internal vesicles (Raiborg et al., 2002). Support for this hypothesis has come from studying the budding of RNA viruses, a ubiquitin-dependent process that is topologically similar to the inward budding of the MVB perimeter membrane. ESCRT-I plays a key role here by recognising a PT/SAP peptide motif within viral proteins (Garrus et al., 2001; Martin-Serrano et al., 2001; VerPlank et al., 2001). This peptide appears to mimic the proline-rich motifs in Hrs that recruit ESCRT-I (Pornillos et al., 2003).

In addition to inward invagination, microscopical studies show that other elaborate changes also occur in the form and distributions of endosome tubules and vacuoles when ligand binding induces EGFR to internalise (Futter et al., 1996). These changes underline the contribution that the morphology of the endosome plays in selectively routing cargo. The importance of partitioning the endosome into tubular and vesicular compartments in order to promote sorting is not restricted to membrane-associated cargo, since these regions also differentially process ligands that dissociate in the low pH of the endosome (Mellman, 1996). Despite its importance, little is known of how the structural organisation of the endosome is achieved. In particular, the relationship between the series of protein-protein interactions that selectively sort trafficking membrane proteins and the membrane shape changes that involve tubulation and vacuolation remain to be determined.

We have used electron microscopy to examine the consequences of inhibiting the processing of EGFR by limiting the levels of TSG101, using RNA interference. In these conditions we find that trafficking EGFR and TR, in addition to fluid-phase content, build up in the early endosome within a compartment that resembles morphologically those described in *S. cerevisiae* mutants defective in ESCRT-I function. In this distinctive compartment the characteristic tubular elements and the vacuoles of early endosomes are no longer identifiable. Instead, it is dominated by distended cisternae held together in folded arrays by an ordered, electron opaque matrix. These observations suggest that Hrs/ESCRT interactions are important for regulating changes in membrane shape and dynamics beyond the sorting of membrane proteins to the MVB.

Materials and Methods

Reagents

The following antibodies were used. Mouse: anti-EEA1 (Transduction Labs); anti-LAMP2 (Developmental Studies Hybridoma Bank, University of Iowa, USA); anti-TR (Zymed); 108 anti-EGFR extracellular domain (J. Schlessinger, New York University Medical Centre, New York, NY, USA); H68.4 anti-TR cytosolic domain (raised in the laboratory of Ian Trowbridge, Salk Institute, San Diego, USA); TAT1 anti-tubulin (Keith Gull, Oxford University, UK); anti-mannose 6-phosphate receptor (ABR); anti-clathrin heavy chain (X22; Elizabeth Smythe, Sheffield University, UK, or clone 23; Transduction Labs). Rabbit: anti-M6PR (Paul Luzio, Cambridge University, UK); anti-golgin84 (a kind gift from Martin Lowe, Manchester University, UK); anti-cathepsin D (DAKO); anti-Hrs (Harald Stenmark, Oslo University, Sweden); anti-lgp120 (Hopkins lab); anti-SNX1 (a kind gift from Matthew Seaman, Cambridge University, UK). HRP (Sigma) was conjugated to Tf using succinimidyl 3-(2-pyridyldithio) propionate (Sigma).

RNA interference

HeLa cells were transfected using standard procedures (Elbashir et al., 2001) as published previously (Bishop et al., 2002). Similar phenotypes were observed using an independent RNA oligonucleotide duplex against TSG101 (Garrus et al., 2001) (data not shown). For controls, cells were transfected in parallel with siRNA for lamin A (Elbashir et al., 2001). Cells were transfected twice, with an interval of 24 hours, and replated 4-6 hours after the second transfection. Experiments were performed 72 hours after the initial transfection. Cells were routinely analysed by western blotting for levels of TSG101 and control proteins. Biochemical experiments were included only when the level of knockdown exceeded an estimated 90%.

Fluorescence microscopy

For EGF uptake, cells were incubated as described previously (Bishop et al., 2002). Secondary antibodies were from Jackson Labs (PA, USA). For Tf uptake, 5 μg/ml Texas Red Tf (Molecular Probes) was bound in binding medium (BM; L-15 medium with 0.2% BSA), then internalised in BM containing 0.1 mg/ml Tf. Cells were examined using a Leica SP2 confocal microscope (63× objective, 2× zoom). Images were processed using Adobe Photoshop 6.0.

Trafficking experiments

To measure cathepsin D transport, cells in 35 mm dishes were incubated with DMEM minus Met/Cys containing 5% dialysed serum for 1 hour at 37°C, followed by 15 minutes in pulse medium (DMEM minus Met/Cys, 20 mM Hepes pH 7.4, 0.25 mg/ml BSA) containing 5 μl EXPRE^{35}S label (NEN; 10 mCi/ml). After three washes in ice-cold PBS, cells were incubated in 1 ml chase medium (pulse medium containing 1 mM cysteine, 1 mM methionine, 2.5 mM mannose 6-phosphate). Medium was removed and then cells lysed for 15 minutes on ice in 500 μl lysis buffer [20 mM Hepes pH 7.4, 150 mM NaCl, 1 mM EDTA, 0.5% (w/v) Triton X-100]. Protease inhibitor cocktail III (Calbiochem) was added to all samples. Samples were immunoprecipitated with anti-cathepsin D and protein A-Sepharose, then run on SDS-PAGE and analysed by autoradiography and phosphorimaging. To measure cycling and degradation of ^{125}I-EGF, cells in 35 mm dishes were incubated with ^{125}I-EGF (50 μCi/μg; 20 ng/ml) in BM for 15 minutes at 37°C. Cells were washed for 5 minutes on ice with 150 mM NaCl, 100 mM glycine pH 3.0 to remove surface-associated radiolabel, and incubated in 1 ml BM at 37°C. Medium was removed at various times as indicated. Half was counted for radioactivity directly (degraded plus recycled); the remainder was precipitated in 10% (w/v) TCA and the supernatant counted for radioactivity (degraded). Cells were lysed in 1 M NaOH to count residual cell-associated radioactivity. Uptake and recycling of ^{125}I-Tf was performed using a deferoxamine wash cycle to remove surface-bound Tf as described previously (Jing et al., 1990).

Electron microscopy

Cells were grown on glass coverslips and preincubated for 1 hour in serum-free medium. They were then incubated at 4°C with or without EGF/anti-EGFR antibody (200 ng/ml Texas Red-streptavidin-biotin-EGF (Molecular Probes) and 108 anti-EGFR antibody directly conjugated to 10 nm gold) for 30 minutes in BM supplemented with 0.5 μM $Fe(NO_3)_3$, washed with L-15 warmed to 37°C and incubated for various times at 37°C. Where indicated, the last 30 minutes of each incubation was with TfHRP (20 μg/ml). For fluid-phase HRP loading, cells were preincubated for 1 hour as above, incubated at 4°C for 30 minutes in L-15 and then at 37°C for 4-8 hours in 5 mg/ml HRP (Sigma) in L-15. With the exception of cells prepared for post-fix immunogold labelling, cells incubated at 37°C were rinsed in PBS and fixed at room temperature for 15 minutes with 2% PFA/1.5%

glutaraldehyde in 100 mM sodium cacodylate, pH 7.5. Fixed cells were then treated with diaminobenzidine (DAB; Sigma) to cross-link HRP (Stinchcombe et al., 1995). For post-fix immunogold labelling, cells incubated at 37°C were rinsed in L-15 and then ascorbic acid buffer (20 mM Hepes, 70 mM NaCl, 50 mM ascorbic acid, pH 7.0) at 4°C and treated with 750 μg/ml DAB and 0.02% H_2O_2 in ascorbic acid buffer to crosslink HRP. The cells were then permeabilised by incubating in 40 μg/ml digitonin in permeabilisation buffer (25 mM Hepes, 38 mM aspartate, 38 mM glutamate, 38 mM gluconate, 2.5 mM $MgCl_2$, 2 mM EGTA, pH 7.2). They were then fixed in 2% paraformaldehyde and returned to room temperature, quenched with 15 mM glycine and 50 mM NH_4Cl and blocked with 1% BSA before indirect immunogold labelling with anti-TR H68.4, anti-SNX1 or anti-lgp120 and secondary antibody conjugated to 5 nm gold (British Biocell International). The cells were then fixed in 2% PFA/1.5% glutaraldehyde and rinsed in 100 mM sodium cacodylate, pH 7.5. All cells were then treated with 1% osmium tetroxide/1.5% potassium ferricyanide and tannic acid before dehydration and embedding on Epon stubs, as described previously (Stinchcombe et al., 1995). The coverslips were removed by immersion in liquid nitrogen. Cells were sectioned en face, stained with lead citrate, and viewed in a Philips EM400 electron microscope. Images were taken from negatives using a Flextight Precision II scanner (Imacon) and processed in Adobe Photoshop 5.0.

Results

Depletion of TSG101 disrupts EGFR transport from the early endosome

We have previously shown that depletion of TSG101 results in a reduction in EGFR degradation as assessed semi-quantitatively by western blotting (Bishop et al., 2002). To more precisely identify the site at which TSG101 acts and gain insight into the underlying reasons for the block in trafficking, we performed a detailed kinetic and morphological analysis. HeLa cells were depleted of TSG101 by RNA interference, conditions that led to almost total loss of TSG101 protein (Fig. 1A). Vacuolar protein sorting 28 (VPS28), an additional component of ESCRT-1 (Babst et al., 2000; Bishop and Woodman, 2001), was also quantitatively depleted in cells lacking TSG101 (Fig. 1A). This suggests that the ESCRT-I complex as a whole is destabilised upon depletion of TSG101. By contrast, little effect was observed on the stability of several upstream and downstream components of the MVB sorting pathway, including Hrs and the ESCRT-III protein VPS24 (data not shown). ^{125}I-EGF degradation over a 3-hour period was reduced by approximately 50% in cells that lacked ESCRT-I compared with that in cells depleted of a control protein, lamin A (Fig. 1B). Depletion of TSG101 was accompanied by only a modest increase in the extent of ^{125}I-EGF recycling. Instead, the population of intracellular, unprocessed ^{125}I-EGF declined in TSG101-depleted cells much more slowly than in control cells, so that after 3 hours internalisation there was a threefold accumulation of ^{125}I-EGF relative to control cells, corresponding to approximately 25% of internalised ligand. These findings are in contrast to earlier studies using mouse fibroblasts that were partially depleted of TSG101 (Babst et al., 2000) where impairment of EGF degradation was largely accounted for by a substantial increase in EGFR recycling. Indeed, the reduction in the cell surface population of EGFR upon TSG101 depletion (see legend to Fig. 1) may be due to impaired recycling of constitutively endocytosed receptor and hence might point to a general reduction in membrane recycling.

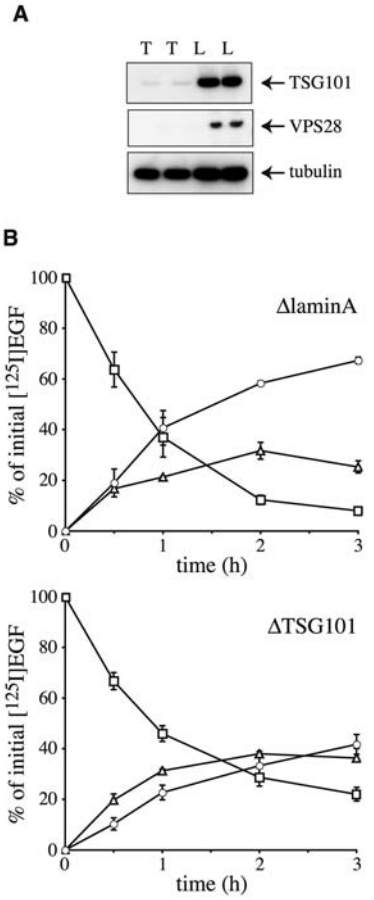

Fig. 1. Depletion of TSG101 causes intracellular retention of undegraded EGF. (A) Duplicate samples of lamin A-depleted (L) or TSG101-depleted (T) cells were lysed in SDS-PAGE sample buffer and analysed by western blotting for TSG101, VPS28, and tubulin. (B) Lamin A-depleted (upper panel) or TSG101-depleted (lower panel) HeLa cells were incubated with ^{125}I-EGF for 15 minutes at 37°C. After a brief wash to remove cell surface ^{125}I-EGF, cells were incubated at 37°C for the indicated times. Samples were analysed for degraded ^{125}I-EGF (circles), undegraded recycled EGF (triangles) and remaining cell-associated ^{125}I-EGF (squares). Note that initial binding of EGF was reduced by 27.4%±10.0% in TSG101-depleted cells. Values are means from three experiments, each performed in duplicate, ± s.e.m.

To identify the site of EGF accumulation we internalised Alexa Fluor488-labelled EGF for 3 hours and examined cells by immunofluorescence microscopy. In control cells, almost no internalised Alexa Fluor488 EGF remained cell-associated, having been either degraded in lysosomes or recycled (data not shown). Immunolabelling of these cells for early endosome-associated antigen 1 (EEA1; Fig. 2A), Hrs (Fig. 2B) or LAMP2 (Fig. 2C) was typical for these markers, indicating that early and late endocytic compartments were not affected by lamin A depletion or by the transfection regime. Essentially identical staining was observed in cells that had not internalised EGF (data not shown).

By contrast, when ESCRT-I was depleted, Alexa Fluor488 EGF was found in clustered structures that were labelled by the early endosome markers EEA1 (Fig. 2D-F) and SNX1 (data not shown). Identical results were obtained using a separate

siRNA oligonucleotide (data not shown). We stained cells for Hrs, which localises to EGFR-enriched domains at the early endosome and which acts immediately upstream of ESCRT-I (Bache et al., 2003a; Raiborg et al., 2002; Sachse et al., 2002). Localisation of Alexa Fluor488 EGF and Hrs was almost completely coincident (Fig. 2G-I). Together, these data suggest that the first site at which TSG101 functions during EGFR trafficking is at the early endosome in the immediate vicinity of Hrs, despite most TSG101 localising to late endosomes and lysosomes at steady state (Bache et al., 2003a). The distribution of EEA1 and Hrs was dramatically different in TSG101-depleted cells compared with control cells, indicating that the trafficking block at the early endosome affected the organisation of this compartment. LAMP2-positive lysosomes were also affected by TSG101 depletion (Fig. 2, compare K and C), with some evidence of enlargement and/or clustering. However, no Alexa Fluor488 EGF associated with these structures (Fig. 2J-L). Hence, the block in EGF degradation is not simply a consequence of the failure to degrade ligand that has been transported normally to the lysosome.

Overexpression of Hrs recruits both clathrin and dynamin to the early endosome (Raiborg et al., 2001), consistent with the localisation of Hrs to clathrin-coated domains of the endosome which specialise in EGFR sorting (Bache et al., 2003a; Sachse et al., 2002). In addition, expression of a dominant-negative VPS4 stabilises clathrin-Hrs domains within the limiting membranes of aberrant endosomes that are deficient in MVB sorting (Sachse et al., 2004). In contrast to these studies, neither clathrin (Fig. 3A-C) nor dynamin (Fig. 3D-F) was routinely detected on Hrs-positive structures containing accumulated EGF in TSG101-depleted cells. Some clathrin did localise to EGF-positive vacuoles in a subset of cells, but the level of labelling was substantially lower than that on endosomal vacuoles in cells expressing dominant-negative VPS4 (data not shown). These data were confirmed using a second antibody that recognises a distinct epitope on clathrin (data not shown).

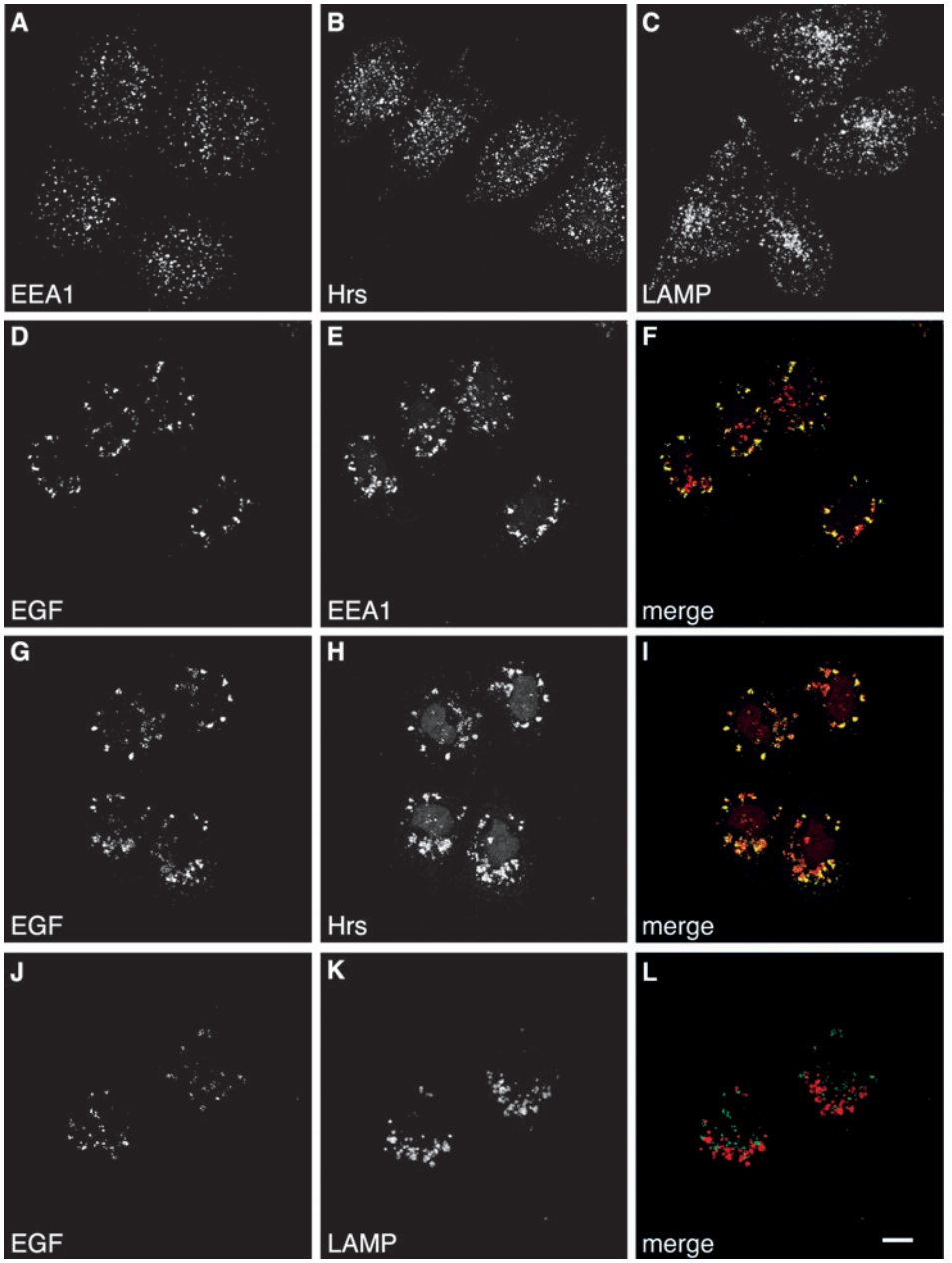

Early endosomes in TSG101-depleted cells do not maintain structural boundaries

We examined the defects in EGF trafficking and early endosome morphology by electron microscopy in order to gain a better understanding of the function of the mammalian ESCRT-I complex (Bache et al., 2003a; Lloyd et al., 2002). One question that we tried to answer is whether depletion of TSG101 would prevent the formation of internal vesicles within MVB, given its functional conservation with the *S. cerevisiae* ESCRT-I component, Vps23p. Importantly, however, detailed

Fig. 2. EGF accumulates in aberrant early endosomes in TSG101-depleted cells. (A-C) Lamin A-depleted HeLa cells were allowed to internalise Alexa Fluor488-labelled EGF for 3 hours and cells were examined by fluorescence microscopy for EEA1 (A), Hrs (B) or LAMP-2 (C) (note that virtually all the Alexa Fluor488-labelled EGF had been lost from cells at this time, and panels showing the residual Alexa Fluor488-labelled EGF are not provided). (D-L) TSG101-depleted cells were allowed to internalise Alexa Fluor488-labelled EGF for 3 hours. Cells were examined by fluorescence microscopy for EGF (D,G,J; green), EEA1 (E; red), Hrs (H; red) or LAMP-2 (K; red). Merged images are shown in F,I,L. Bar, 10 μm.

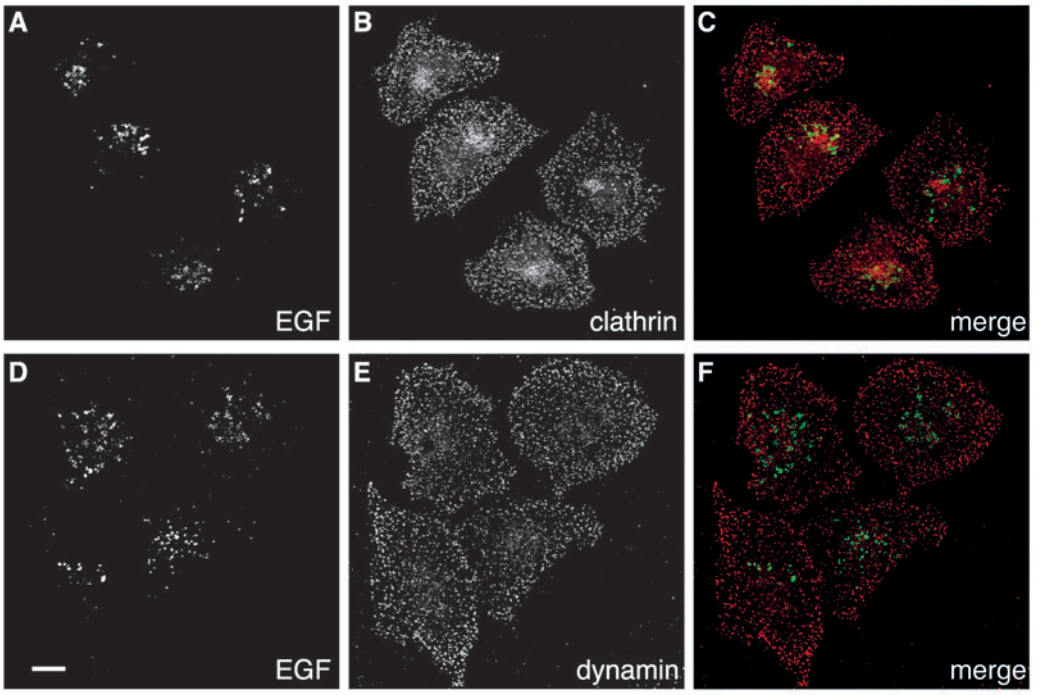

Fig. 3. Clathrin and dynamin do not associate with aberrant early endosomes induced by TSG101 depletion. TSG101-depleted HeLa cells were allowed to internalise Alexa Fluor488-labelled EGF for 3 hours at 37°C. Cells were fixed and examined by fluorescence microscopy for EGF (A,D; green), clathrin (B; red) or dynamin (E; red). Merged images are shown in C and F. Bar, 10 μm.

morphological examination and immunogold labelling should provide additional clues about the activity of ESCRT-I during receptor sorting. In particular, it was important to establish if receptor sorting within the endosomal membrane would still occur in the absence of TSG101, since ESCRT-I is believed to act downstream of Hrs- and clathrin-dependent cargo selection (Bache et al., 2003a).

Trafficking of EGFR was followed using a gold-conjugated antibody to the receptor external domain (108 gold). Bound 108 gold is internalised as a consequence of EGF uptake, thereby allowing examination of the distribution of EGFR (Futter et al., 1996). Compartments within the early endosome pathway were identified by loading cells with TfHRP to steady state. Studies on control cells (untreated with RNAi) have shown these compartments include 100 nm diameter tubules containing TfHRP, which are often continuous with small (0.1-0.2 μm diameter) vacuoles containing only one or two 30-50 nm diameter vesicles. Larger (0.2-0.4 μm diameter) vacuoles containing only trace levels of TfHRP also form in response to EGF/EGFR internalisation. In these vacuoles the number of internal vesicles may eventually increase to fill virtually all the available lumenal space, and most of the internalised EGFR-gold label is on the internal vesicles. On the cytosolic surfaces of these vacuoles discrete coated patches are frequently observed (data not shown). These are identical to domains shown to contain both clathrin heavy chain and Hrs (Sachse et al., 2002).

In RNAi-treated cells in which TSG101 has been significantly reduced, the early endosome compartments (identified by their content of TfHRP) are dominated by a new subset of vacuolar structures that appear to develop at the expense of the tubules and vacuoles seen in control cells (in cells displaying these vacuoles normal early endosomes and MVB are almost never seen; data not shown). The most prominent of these structures are folded cisternae with wide lumena that closely resemble the compartment observed in *S. cerevisiae* Class E vps mutants (Raymond et al., 1992; Rieder et al., 1996) (Fig. 4A). Between the folds of the cisternae is a finely fibrous, electron opaque matrix within which crossbridging structures are evident (Fig. 4A, arrows). No other surface elaborations are apparent. In particular, the characteristic clathrin bristle coat that is observed in untreated cells and which dominates the membrane when ESCRT-III is disrupted by expressing a dominant-negative VPS4 mutant (Sachse et al., 2004) is absent (see Fig. 4A). The lumena of the cisternae seldom contain internal vesicles, although some invaginations/internal vesicles can be identified at cisternal ends, which are slightly dilated. EGFR-108 gold internalises to the limiting membranes of these structures within 10-15 minutes of it being endocytosed (data not shown), and is held for as long as 3 hours (Fig. 4B).

Some TSG101-depleted cells contained an additional feature instead of the multi-cisternal structures: large electron lucent vacuoles that label with DAB reaction product at the limiting membrane and in adjacent tubules and vesicles (Fig. 4C). Multicisternal endosomes and normal endosomes/MVBs were absent from cells containing these vacuoles. These

Table 1. Density of SNX1 immunogold labelling over multicisternal endosomes

	Lamin A siRNA	TSG101 siRNA
Membrane (μm)	15.46	16.71
Total SNX1 particles	59	57
Particles per μm membrane	3.8	3.4

Lamin A- or TSG101-depleted cells were incubated with Tf-HRP for 45 min at 37°C and post-fix labelled with 5 nm gold for SNX1. Measurements were made of membrane length of Tf-HRP-containing endosomes in control cells (from 6 cells) and Tf-HRP-containing multicisternal endosomes from TSG101-depleted cells (7 cells; only membrane exposed to cytosol was measured, based on the assumption that antibody would be excluded from intercisternal areas). SNX1 gold particles on measured membrane were counted.

structures retain some ability to sort cargo, since Tf-HRP often becomes restricted to adjacent tubules/vesicles whilst EGFR-108 gold remains within the vacuoles after 3 hours of EGFR internalisation (data not shown). The characteristic matrix is also often seen at regions where vacuoles abut each other (data not shown). For these reasons we believe that these vacuoles are related to cisternae, either as precursors or as an intermediate structure. However, attempts to demonstrate this using RNAi time-course experiments were inconclusive (data not shown), and the loss of vacuoles when cells were treated with digitonin likewise prevented their further analysis. The endosomal system of lamin A-depleted cells is essentially identical to untreated cells, with TR-containing tubules (see Fig. 8C) and vacuoles that develop into MVB that efficiently transport EGFR to lysosomes (Fig. 4D,E).

We have performed dual labelling experiments with EGFR-108 gold and early or late endocytic markers in order to provide further information about the multicisternal endosomes found in TSG101-depleted cells. For these experiments, cells were incubated with digitonin prior to fixation in order to permeabilise the plasma membrane and allow antibody to access the cytosolic face of structures. As expected, cisternae containing EGFR-108 gold label for Hrs (Fig. 5A). Cisternae also label for SNX1 (Fig. 5B), a marker of both tubular and vacuolar regions of the early endosome in control cells (Seaman, 2004) (Fig. 5C). Importantly, the density of SNX1 labelling over cisternae is virtually identical to that which occurs over early endosomes in control cells (Table 1). By

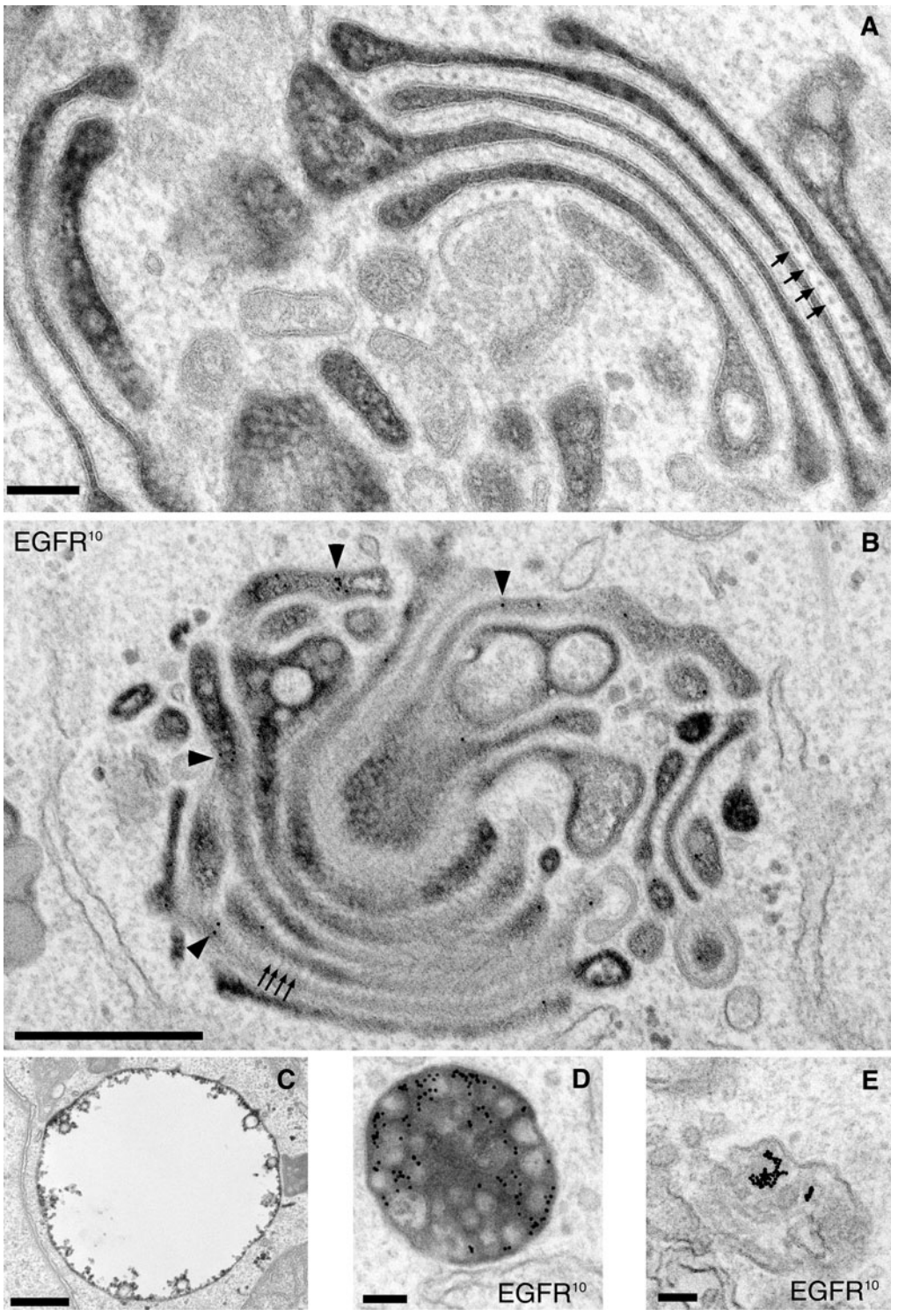

Fig. 4. Morphology of multicisternal early endosomes in TSG101-depleted cells. TSG101-depleted HeLa cells were incubated with TfHRP for 30 minutes to label early endosomes (A,C), or incubated with EGF and 108 anti-EGFR 10 nm gold for 30 minutes at 4°C, washed, and incubated at 37°C for a further 3 hours, with TfHRP added for the final 30 min (B; note that in this oblique section the inter-cisternal matrix appears as striations). Arrowheads indicate anti-EGFR gold. Arrows indicate matrix. Lamin A-depleted HeLa cells were incubated with EGF and 108 anti-EGFR 10 nm gold for 30 minutes at 4°C, washed, and incubated at 37°C for a further 30 minutes (D) or 3 hours (E). For the final 30 min the cells were incubated with Tf-HRP. Electron dense content; cross linked Tf-HRP. Bars, 0.1 μm (A,D,E); 0.5 μm (B,C).

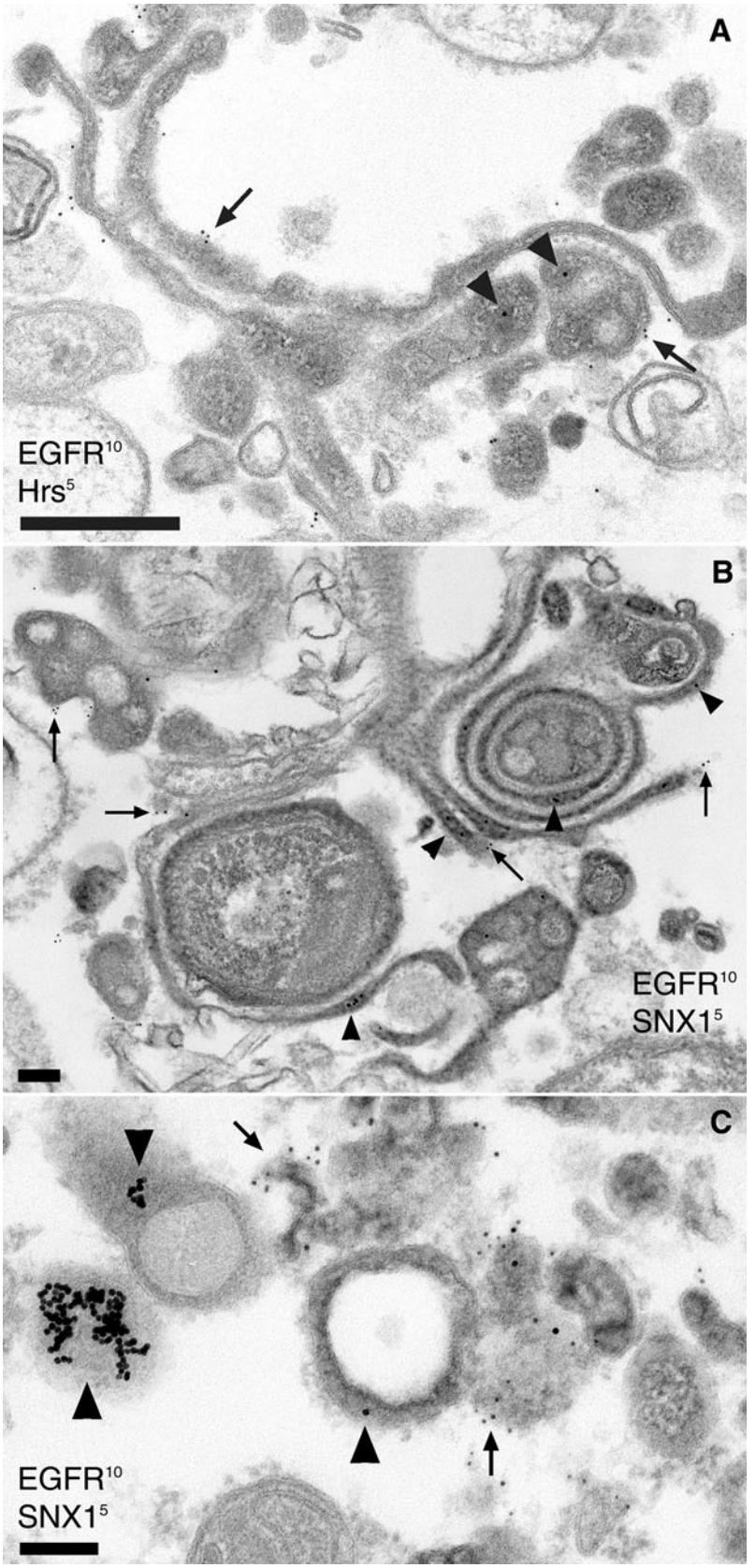

Fig. 5. Hrs and SNX1 localise to multicisternal endosomes. TSG101-depleted (A,B) and lamin A-depleted (C) HeLa cells were incubated with EGF and 108 anti-EGFR 10 nm gold for 30 minutes at 4°C, washed, and incubated at 37°C for a further 1 hour (for the experiment showing Hrs labelling) or 3 hours (for the experiment showing SNX1), with TfHRP added for the final 30 minutes. The cells were then post-fix labelled with 5 nm gold for Hrs (A) or SNX1 (B, C). Arrowheads indicate anti-EGFR-gold; arrows indicate anti-Hrs-gold or anti-SNX1-gold. Bars, 0.5 μm (A); 0.1 μm (B,C).

contrast, multicisternal endosomes contain low levels of the lysosomal marker lgp120, which is found on lysosomes at the same membrane density in control and TSG101-depleted cells (Fig. 6 and Table 2). In summary, these data reveal that cisternae are derived almost exclusively from early endosomes and do not contain significant levels of lysosomal membrane.

Despite the clearly differentiated membrane content of multicisternal endosomes and lysosomes in TSG101-depleted cells, we observed many instances where cisternae and lysosomes abut each other with the characteristic fibrous matrix in between. No mixing of membrane content (TR, EGFR, lgp120) occurs, even where the interconnections are extensive (Fig. 6A). Consistent with this, in cells containing multicisternal endosomes, most of the internalised EGFR-108 gold does not reach lysosomes even after a 3-hour chase (Table 3, Fig. 7A). It is also noteworthy that whilst fluid phase HRP will load the folded endosomal cisternae it, too, fails to reach the lysosome during a continuous and extended pulse (contrast Fig. 7B,C). In addition, BSA-gold reached multicisternal endosomes during a 30 minute pulse and remained in these structures during a subsequent 4-hour chase (data not shown).

MVB formation is preceded by selection of EGFR into Hrs-enriched clathrin-coated domains of the endosome. Since TSG101 acts downstream of Hrs (Bache et al., 2003a), one might expect that impairment of EGFR trafficking from multicisternal endosomes in TSG101-depleted cells occurs at a point after receptor sorting, so that EGFR and TR become separated but can no longer move to morphologically distinct compartments. Indeed, clathrin-dependent sequestration of EGFR proceeds as normal when ESCRT-III function is impaired by expression of a dominant-negative form of VPS4 (Sachse et al., 2004). Importantly, however, immunogold labelling shows that TR and EGFR are co-distributed within the multicisternal endosome with no regions that are obviously enriched for EGFR (Fig. 8A), though some TR labelling is also found on neighbouring tubular-vesicular membranes which appear to lack EGFR. As expected, TR and EGFR do not co-localise and are associated with morphologically distinct membranes in control cells (Fig. 8B,C).

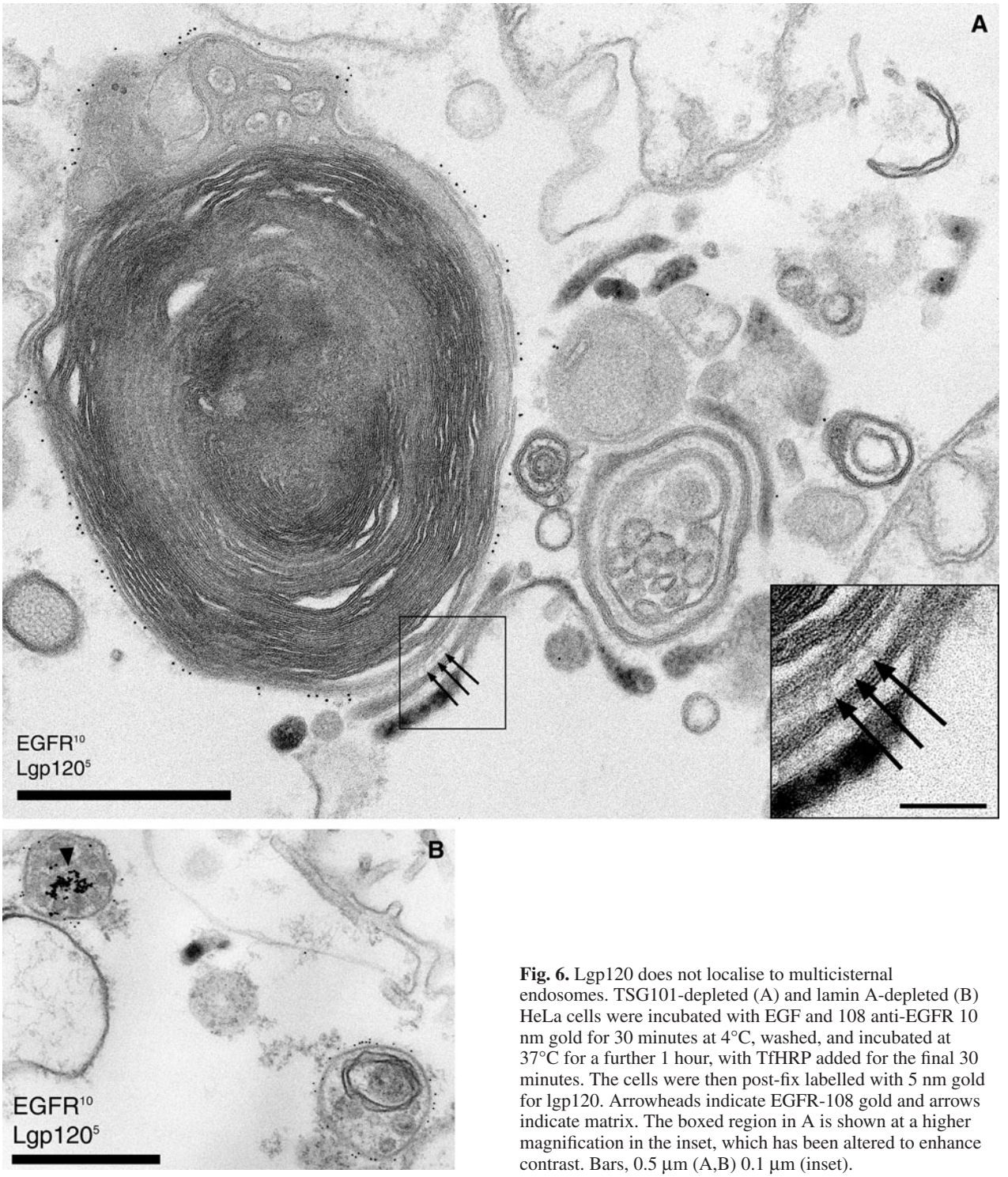

Fig. 6. Lgp120 does not localise to multicisternal endosomes. TSG101-depleted (A) and lamin A-depleted (B) HeLa cells were incubated with EGF and 108 anti-EGFR 10 nm gold for 30 minutes at 4°C, washed, and incubated at 37°C for a further 1 hour, with TfHRP added for the final 30 minutes. The cells were then post-fix labelled with 5 nm gold for lgp120. Arrowheads indicate EGFR-108 gold and arrows indicate matrix. The boxed region in A is shown at a higher magnification in the inset, which has been altered to enhance contrast. Bars, 0.5 μm (A,B) 0.1 μm (inset).

Multiple post-endosomal sorting pathways are disrupted by TSG101 depletion

Given that depletion of TSG101 disrupts cargo selection, we examined the extent to which other transport pathways through the early endosome are affected. The precursor to the lysosomal hydrolase cathepsin D is transported between the TGN and an endosomal compartment via the mannose 6-phosphate receptor (M6PR). An intermediate form is generated by cleavage of the precursor within the late endosome, followed by processing to the mature protease within the lysosome (for a review, see Ghosh et al., 2003). In contrast to control cells, in which cathepsin D was processed in full within 4 hours chase, limited processing to the intermediate and mature forms occurred in TSG101-depleted cells (Fig. 9A,B). These data indicate that cathepsin D transport is blocked in a mildly proteolytic environment and/or has failed to reach a

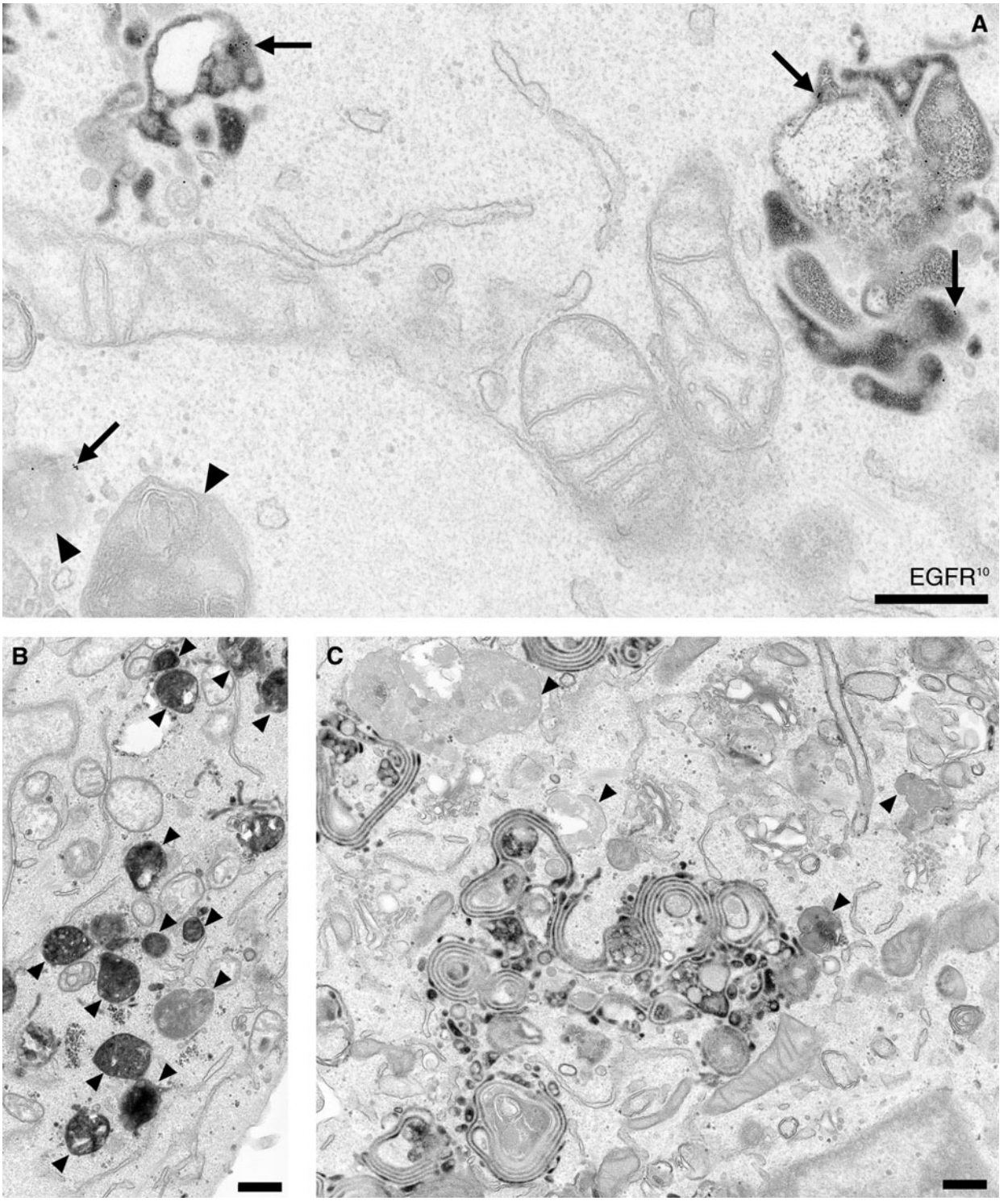

Fig. 7. Transport to lysosomes is impaired in TSG101-depleted cells. (A) TSG101-depleted HeLa cells were incubated with EGF and 108 anti-EGFR 10 nm gold for 30 minutes at 4°C, washed, and incubated at 37°C for a further 3 hours, with TfHRP added for the final 30 minutes. Examples of EGFR-gold complexes are indicated by arrows. (B,C) Lamin A-depleted control (B) or TSG101-depleted (C) HeLa cells were incubated for 8 hours with fluid-phase HRP at 37°C. Similar results were obtained after 4 and 6 hours (not shown). Electron dense content is crosslinked HRP. Lysosomes (based on morphology) are indicated by arrowheads. Bars, 0.5 μm.

compartment that is sufficiently acidic to permit cathepsin D autoprocessing. The increase in secretion of newly synthesised cathepsin D likewise suggests that the population of unoccupied M6PR within the TGN is reduced. Indeed, M6PR almost completely colocalised with EEA1 within TSG101-depleted cells (Fig. 9C, centre panels), in contrast to its

Table 2. Density of lgp120 immunogold labelling over endosomes and lysosomes

Tf-HRP endosomes	Lamin A siRNA	TSG101 siRNA
Membrane (μm)	14.07	16.11
Total lgp120 particles	9	17
Particles per μm membrane	0.6	1.1
Lysosomes	**Lamin A siRNA**	**TSG101 siRNA**
Membrane (μm)	14.32	16.11
Total lgp120 particles	237	268
Particles per μm membrane	16.6	16.6

TSG101-depleted and lamin A-depleted cells were incubated with EGF and 108 anti-EGFR 10 nm gold for 30 minutes at 4°C, washed, and incubated at 37°C for a further 1 hour, with TfHRP added for the final 30 minutes. The cells were then post-fix labelled with 5 nm gold for lgp120. Measurements were made of membrane length of Tf-HRP-containing endosomes and of lysosomes (scored by morphology; heterogeneous content, and single perimeter membrane containing at least one lgp120 gold particle) in control cells (from 6 cells) and of Tf-HRP-containing multicisternal endosomes and of lysosomes from TSG101-depleted cells (6 cells; only membrane exposed to cytosol was measured, based on the assumption that antibody would be excluded from intercisternal areas). Lgp120 gold particles on measured membrane were counted.

Table 3. Loss of ESCRT-I disrupts transport of EGFR to the lysosome

Lamin-A RNAi (from 9 cells)				
	Lysosomes	MVBs	Unclassified	Autophagosomes
108 particles	1515	35	169	19
Percentage of total (1738)	87.2	2.0	9.7	1.1

TSG101 RNAi (from 10 cells containing MC structures)				
	Lysosomes	Cisternae	Unclassified*	Autophagosomes
108 particles	50	272	296	54
Percentage of total (672)	7.4	40.5	44.0	8.0

HeLa cells were incubated with EGF and 108 anti-EGFR 10 nm gold for 30 minutes at 4°C, washed, and incubated at 37°C for a further 3 hours, with TfHRP added for the final 30 minutes. Gold particles were counted in classes of intracellular membranes; lysosomes, MVBs and autophagosomes were scored by morphology. Cisternae were scored as endosomes containing TfHRP in part of a matrix-linked structure.

*Note that in TSG101 cells many 'unclassified' structures were small TfHRP-containing structures close to multicisternae, and were probably linked to them outside the plane of the section.

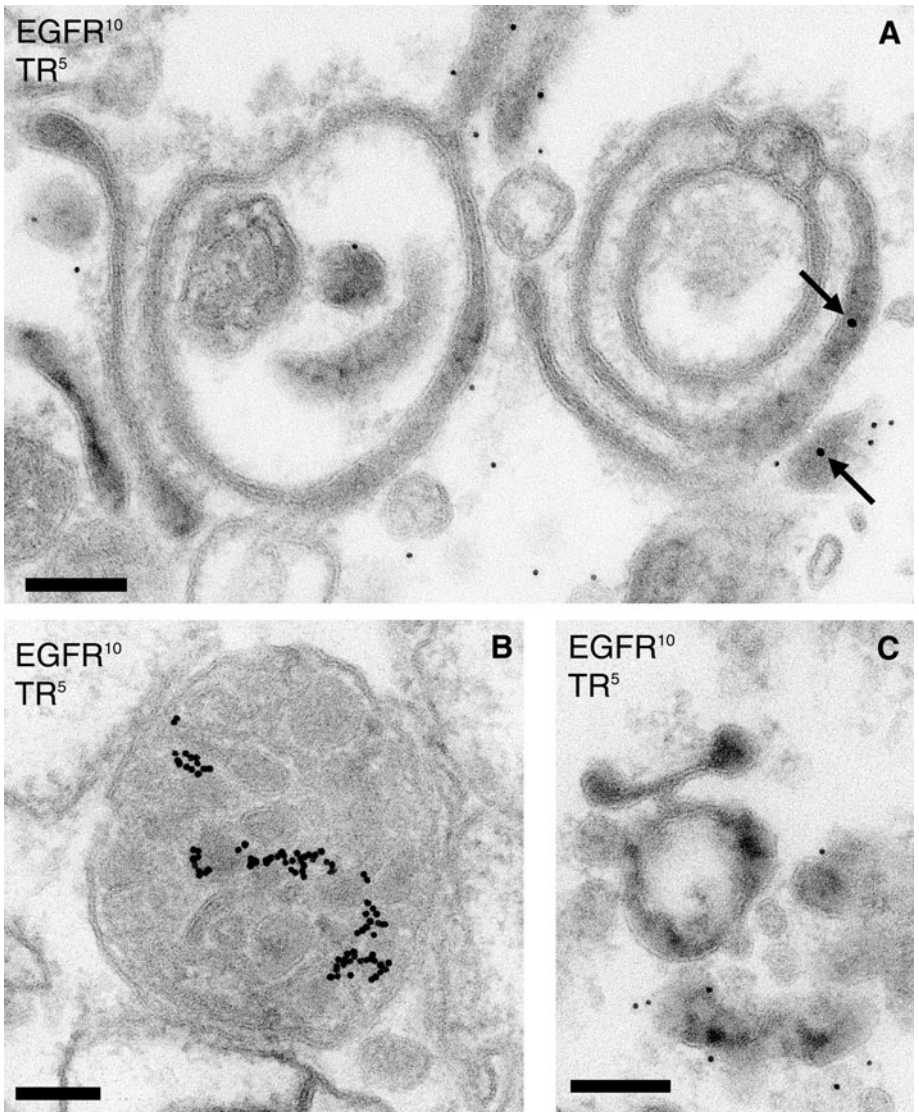

localisation in control cells where it is concentrated in the region of the Golgi complex as well as being found in peripheral structures (Fig. 9C, upper panels). In addition, M6PR was located within EGF-positive compartments after prolonged incubation of cells with Alexa Fluor488 EGF (Fig. 9C, lower panels). Therefore, Class E early endosomes are defective in retrieval of membrane to the TGN. Consistent with this, TSG101 depletion caused a marked redistribution of TGN46, but not Golgin-84 [a component of the Golgi stack (Diao et al., 2003)], from the Golgi region (Fig. 10A, panels A-F). The precise localisation of TGN46 could not be determined because of the extensive dilution of antigen away from the TGN.

Multicisternal endosomes became labelled with Tf-HRP, indicating that some receptor could transit between the

Fig. 8. EGFR and TR colocalise to aberrant early endosomes. TSG101-depleted (A) and lamin A-depleted (B,C) HeLa cells were incubated with EGF and 108 anti-EGFR 10 nm gold for 30 minutes at 4°C, washed, and incubated at 37°C for a further 1 hour, with TfHRP added for the final 30 minutes. The cells were then post-fix labelled with 5 nm gold for TR. Note that B and C are from the same cell labelled for EGFR and TR and show the separate localisations of EGFR (B) and TR (C). EGFR-108 gold complexes are indicated by arrows (10 nm gold). Bars, 0.1 μm.

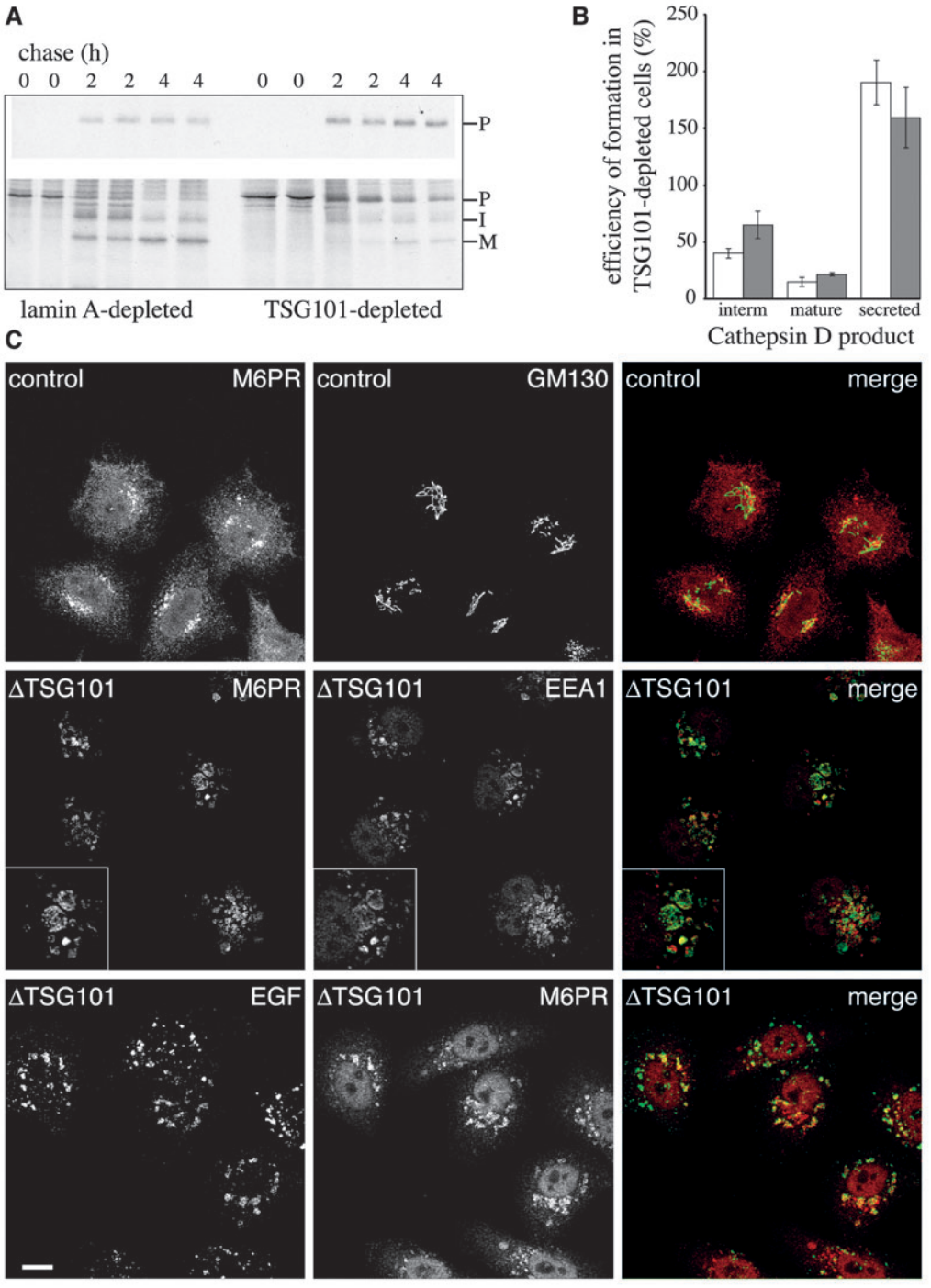

Fig. 9. Depletion of TSG101 disrupts trafficking of lysosomal precursors at the early endosome. (A) Lamin A or TSG101-depleted HeLa cells were pulse labelled with [^{35}S]methionine and chased as indicated in the presence of excess unlabelled methionine. Anti-cathepsin D immunoprecipitates from cell culture supernatants (top part) and cells (bottom part) were analysed by SDS-PAGE and fluorography. The migration positions of procathepsin D (P; 45 kDa), the intermediate cleaved form of cathepsin D (I; 40 kDa) and mature cathepsin D (M; 27 kDa) are indicated. Duplicate samples from a representative experiment are shown. (B) Phosphorimager data from cathepsin D pulse-chase experiments were analysed to determine the amounts of cathepsin D cleaved to the intermediate form (interm), cleaved to the mature form (mature) or secreted from cells (secreted) in TSG101-depleted cells relative to lamin A-depleted cells. Data from a 2-hour chase are shown as white bars, and those from a 4-hour chase as shaded bars. Data are the means ± s.e.m. from three independent experiments, each performed in duplicate. (C) Lamin A-depleted (upper panels) or TSG101-depleted (centre panels) cells were fixed and stained for mannose 6-phosphate receptor (M6PR; green), and GM130 or EEA1 (red) as indicated. Inserts are magnified twofold relative to the main images. Alternatively, TSG101-depleted cells (lower panels) were allowed to internalise Alexa Fluor488-labelled EGF for 3 hours at 37°C prior to fixation, then examined for EGF (green) and mannose 6-phosphate receptor (red). Bar, 10 μm.

cell surface and endosome after TSG101 knockdown. However, significant redistribution of TR occurred, with a reduction in cell surface labelling and consequent increased staining of enlarged endosomes that labelled for internalised EGF (Fig. 10A, panels G-L). To provide more detailed information about how TR trafficking is affected by loss of TSG101 we labelled cells with ^{125}I-Tf and followed a single round of Tf internalisation and recycling. Control and TSG101-depleted cells did not differ greatly in the rate at which a single round of surface-bound Tf was subsequently internalised and recycled (Fig. 10B upper panel). However, the amount of receptor at the cell surface available for Tf binding was markedly reduced in cells lacking TSG101 (Fig. 10B lower panel), even though the total complement of TR was unaffected (Fig. 10C). Consistent with this, uptake of fluorescently labelled Tf was also reduced (Fig. 10D). These data contrast with previous experiments, which failed to observe a defect in TR cycling when TSG101 levels were reduced to a more limited extent (Babst et al., 2000), or shortly after ESCRT-I function was inhibited acutely by microinjection of antibodies (Bishop et al., 2002).

In summary, these data are consistent with the primary site of ESCRT-I function being in the selection of cargo destined to enter intralumenal vesicles within the vacuolar region of the

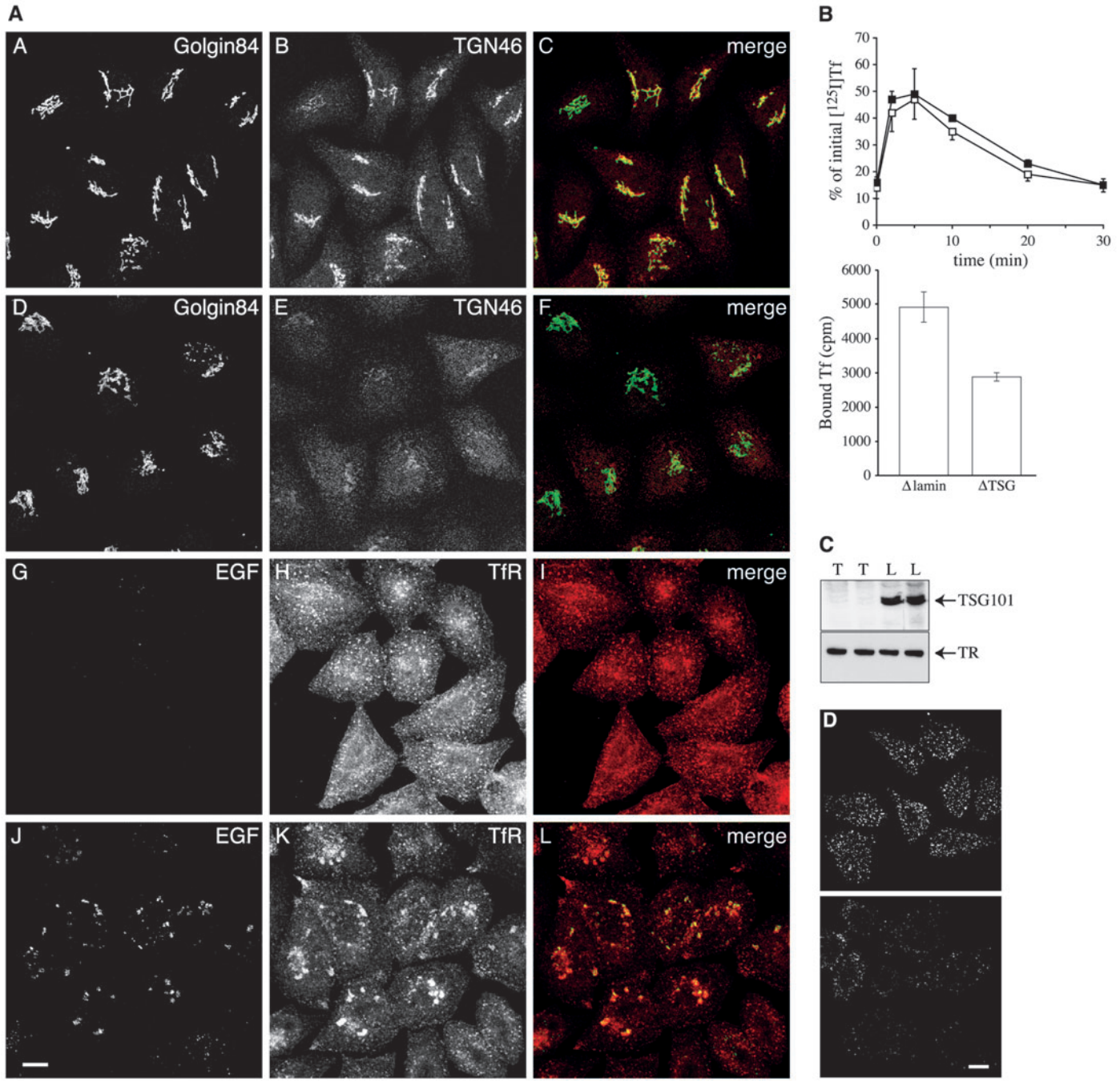

Fig. 10. Recycling pathways to the TGN and plasma membrane are disrupted by TSG101 depletion. (A) Lamin A-depleted (panels A-C,G-I) or TSG101-depleted (panels D-F,J-L) HeLa cells were fixed directly (A-F) and stained for Golgin-84 (green; A,D) and TGN46 (red; B,E), or allowed to internalise Alexa Fluor488-labelled EGF for 3 hours at 37°C prior to fixation (G-L), then examined by fluorescence microscopy for EGF (green; G,J) and transferrin receptor (red; H,K). Merged images are shown in panels C,F,I,L. Bar, 10 μm. (B) Upper panel: ^{125}I-Tf was bound to lamin A-depleted or TSG101-depleted HeLa cells for 30 minutes at 4°C, after which the cells were washed to remove unbound material and warmed to 37°C in the presence of excess unlabelled Tf for the indicated times. Cells were chilled on ice and washed with a deferoxamine cycle to remove residual surface-bound Tf before being extracted in 1 M NaOH and counted for radioactivity. Results are expressed as the percentage of Tf that remained cell associated relative to that which had been initially bound. Results are the means from two experiments each performed in duplicate ± s.d. Lower panel: results (expressed as cpm ± s.d.) from samples to which ^{125}I-Tf was bound at 4°C but not subjected to a deferoxamine wash. (C) Lamin A-depleted (L) or TSG101-depleted (T) HeLa cells were western blotted for TSG101 and TR. (D) Control (upper panel) and TSG101-depleted (lower panel) cells were incubated with Texas red-conjugated Tf for 60 minutes at 4°C followed by 5 minutes at 37°C, then fixed and examined by confocal microscopy. The photomultiplier and image analysis settings were identical in both samples. Bar, 10 μm.

early endosome. Importantly, however, they show how disruption of the ESCRT-I sorting complex affects the functional integrity of the early endosome by interfering with its ability to maintain structural boundaries. Consequently, the dramatic change in the morphology of the early endosome caused by loss of ESCRT-I function is accompanied by kinetic defects in multiple trafficking pathways.

Discussion

Previous studies in *S. cerevisiae* have shown that the proteins in the ESCRT-I complex, along with other Class E VPS gene products, are required for trafficking proteins to reach the vacuole lumen (Katzmann et al., 2002; Odorizzi et al., 1998). Class E vps mutants also show an altered phenotype in which whorls of endosomal cisternae develop (Babst et al., 1997; Rieder et al., 1996), and it seems that many of the trafficking pathways traversing the endosome compartment in these mutants are inhibited (Nothwehr et al., 1996; Piper et al., 1995; Raymond et al., 1992; Rieder et al., 1996). Our data, using mammalian cells, are similar in that they suggest that induction of multicisternal endosomes by loss of ESCRT-I is associated with defects in recycling via the endosome from the biosynthetic pathway, though we find that forward trafficking from the compartment is more profoundly affected than is the case in *S. cerevisiae*. Studies have usually concluded that in *S. cerevisiae* the cisternal structures induced are derived from pre-vacuolar elements [though inhibition of transport from an early endosome has been reported (Zahn et al., 2001)]. Our observations at both the light and electron microscope levels suggest, instead, that the cisternal structures that TSG101 knockdown induces are early endosomes (the slight rise in lgp120 content within these structures over that seen in early endosomes from untreated cells is most likely accounted for by the block in anterograde trafficking of biosynthetic cargo). Consistent with this, we also report that recycling to the cell surface is affected by depletion of TSG101. Internalised TR normally enters and recycles both from small tubules and vesicles in the cell periphery and from vacuolar early endosomes, which also contain EGFR. Collectively our kinetic and morphological data suggest that TR may continue to recycle effectively from tubulo-vesicular regions, whilst recycling from vacuolar regions (which give rise to the multicisternal endosomes) is more substantially affected. Additionally, defective forward transport of activated EGFR causes its intracellular retention rather than enhanced recycling, and the reduced binding of EGF to TSG101-depleted cells suggests that recycling of the unoccupied receptor is likewise impaired.

Our studies indicate how the multicisternal endosomes develop by revealing a regularly repeated matrix which interleaves between cisternal folds. The packing of the cisternae, which is presumably caused by extension of this matrix, is reminiscent of Golgi stacks, although it is clear that in many cases the lumena of the endosome structures are continuous rather than being composed of separate cisternae as in the Golgi. Nevertheless, it seems likely that the matrix that develops in the absence of TSG101 includes long chain tethering molecules as found in the Golgi stack matrix (Gillingham and Munro, 2003). In less extreme circumstances, when the mechanisms regulated by TSG101 are operational, these components also probably play a role in tethering and determine the spatial distribution of endosomal elements.

Indeed, our findings suggest that the matrix arises at points where membrane fusion is disrupted and hence its components may normally participate in fusion reactions. Similar ordered matrices have been described previously (Futter et al., 1996), though these were seen at non-productive docking sites between late endosomes and lysosomes and between lysosomes. Particularly striking is the presence of the matrix at regions of juxtaposition between aberrant early endosomes and lysosomes. We believe that the cisternae may similarly derive from homotypic docking reactions involving early endosomes. In the light of this it is intriguing that the Class C/HOPS complex acts as a tethering factor during both late endosome-lysosome and early endosome fusion (Richardson et al., 2004). However, TSG101 depletion does not result in the redistribution of HOPS components to the membrane fraction and we have failed to identify significant changes in the size distribution of HOPS components that might signal a molecular rearrangement or association. Similarly, we have not observed any changes in the biochemical behaviour of the early endosomal tethering factor EEA1.

The near-absence of internal vesicles within these folded cisternae is in keeping with the view that the ESCRT-I complex, and in particular the binding of TSG101, is involved in the production of these vesicles. A key question, however, is why depletion of ESCRT-I exerts such a wide-ranging effect on early endosome morphology and dynamics, since this is not seen when endosomal pathways are disrupted by other interventions. One clue comes from comparing our work with earlier studies from our laboratory, which examined how impairment of phosphatidylinositol 3-kinase activity disrupts EGFR trafficking (Futter et al., 2001). In this situation, the selection of cargo within the MVB limiting membrane continued, even though inward vesiculation was prevented. Under these conditions TR continued to be dispersed to surrounding tubules and the aberrant organelle could still deliver membrane to the lysosome. Hence, formation of intralumenal vesicles per se is not essential for other aspects of endosome function. By contrast, the critical activity of ESCRT-I that we have uncovered is the sequestration of cargo, since EGFR remain within the same membrane as TR for at least 3 hours after internalisation.

In this respect it is of interest that the EGFR-containing multicisternal structures label for Hrs, yet lack clathrin-coated domains. Hence, Hrs may bind to ubiquitinated cargo but be unable to sequester it efficiently in the absence of the scaffold that clathrin would otherwise provide. Hrs binds clathrin directly in vitro and, in response to over expression of Hrs the extent of the clathrin coating is greatly increased (Raiborg et al., 2001). However, our findings imply that ESCRT-I is necessary for endosomally associated native Hrs to bind clathrin during EGFR sorting, possibly by ensuring that the clathrin binding motif within Hrs is exposed. Interestingly, this motif is at the extreme C terminus of Hrs and is preceded by an extensive proline/glutamine-rich region that is likely to act as an unstructured linker region. It is predominantly to this region that TSG101 binds (Bache et al., 2003a; Pornillos et al., 2003). Our interpretation is consistent with recent findings that expression of a dominant-negative mutant of VPS4, which acts downstream of ESCRT-I, impairs MVB formation yet results

in selective enrichment of EGFR into extensive clathrin-rich domains at the early endosome (Sachse et al., 2004). Under these conditions, binding to the endosome of both ESCRT-I and Hrs is enhanced (Bache et al., 2003b; Bishop and Woodman, 2001), and thus the ability of Hrs to interact with clathrin would be more likely maintained.

In summary, the most straightforward interpretation of our data is that, in the absence of TSG101, Hrs/ESCRT complexes cannot form, and ubiquitinated proteins such as EGFR cannot be recruited to, and stably held by, them. In these circumstances the membrane reorganisations required to form an endosome vacuole and its attendant tubules do not properly develop. The delivery of internalised tracers to these structures shows that the delivery of trafficking proteins from the cell surface does continue, and the extensive amount of membrane in these structures suggests that they also continue to receive contributions of membrane from upstream locations. Our interpretation contrasts with data from recent experiments in which phosphatidylinositol 3-kinase activity was inhibited, which suggested that whilst the delivery of EGFR to the lysosome was prevented, delivery of fluid phase content continued (Petiot et al., 2003). Our data would suggest that the phosphoinositide-protein and protein-protein interactions that occur in the early endosome and trap ubiquitinated trafficking proteins into Hrs/ESCRT 1 complexes are also integral to the modelling of membrane boundaries. This modelling is presumably required to produce the vacuoles and tubules that promote ligand dissociation and receptor recycling.

A.D., P.W. and C.R.H. are supported by the MRC (Grants G9722026, G0001128 and G0000470). M.R.G.R. is supported by the BBSRC. We thank Mike Shaw (University of Oxford) for initial experiments. We thank our colleagues for their generous gifts of reagents. We are grateful to members of the Hopkins lab for helpful discussions.

References

Babst, M., Sato, T. K., Banta, L. M. and Emr, S. D. (1997). Endosomal transport function in yeast requires a novel AAA-type ATPase, Vps4p. *EMBO J.* **16**, 1820-1831.

Babst, M., Odorizzi, G., Estepa, E. J. and Emr, S. D. (2000). Mammalian tumor susceptibility gene 101 (TSG101) and the yeast homologue, Vps23p, both function in late endosomal trafficking. *Traffic* **1**, 248-258.

Bache, K. G., Brech, A., Mehlum, A. and Stenmark, H. (2003a). Hrs regulates multivesicular body formation via ESCRT recruitment to endosomes. *J. Cell Biol.* **162**, 435-442.

Bache, K. G., Raiborg, C., Mehlum, A. and Stenmark, H. (2003b). STAM and Hrs are subunits of a multivalent ubiquitin-binding complex on early endosomes. *J. Biol. Chem.* **278**, 12513-12521.

Bilodeau, P. S., Winistorfer, S. C., Kearney, W. R., Robertson, A. D. and Piper, R. C. (2003). Vps27-Hse1 and ESCRT-I complexes cooperate to increase efficiency of sorting ubiquitinated proteins at the endosome. *J. Cell Biol.* **163**, 237-243.

Bishop, N. and Woodman, P. (2001). Tsg101/mammalian vps23 and mammalian vps28 interact directly and are recruited to vps4-induced endosomes. *J. Biol. Chem.* **276**, 11735-11742.

Bishop, N., Horman, A. and Woodman, P. (2002). Mammalian class E vps proteins recognize ubiquitin and act in the removal of endosomal protein-ubiquitin conjugates. *J. Cell Biol.* **157**, 91-102.

Diao, A., Rahman, D., Pappin, D. J. C., Lucocq, J. and Lowe, M. (2003). The coiled-coil membrane protein golgin-84 is a novel rab effector required for Golgi ribbon formation. *J. Cell Biol.* **160**, 201-212.

Elbashir, S. M., Harborth, J., Lendeckel, W., Yalcin, A., Weber, K. and Tuschl, T. (2001). Duplexes of 21-nucleotide RNAs mediate RNA interference in cultured mammalian cells. *Nature* **411**, 494-498.

Felder, S., Miller, K., Moehren, G., Ullrich, A., Schlessinger, J. and Hopkins, C. R. (1990). Kinase activity controls the sorting of the epidermal growth factor receptor within the multivesicular body. *Cell* **61**, 623-624.

Futter, C. E., Pearse, A., Hewlett, L. J. and Hopkins, C. R. (1996). Multivesicular endosomes containing internalized EGF-EGF receptor complexes mature and then fuse with lysosomes. *J. Cell Biol.* **132**, 1011-1023.

Futter, C. E., Collinson, L. M., Backer, J. M. and Hopkins, C. R. (2001). Human VPS34 is required for internal vesicle formation within multivesicular endosomes. *J. Cell Biol.* **155**, 1251-1108.

Garrus, J. E., von Schwedler, U. K., Pornillos, O. W., Morham, S. G., Zavitz, K. H., Wang, H. E., Wettstein, D. A., Stray, K. M., Côté, M., Rich, R. L. et al. (2001). Tsg101 and the vacuolar protein sorting pathway are essential for HIV-1 budding. *Cell* **107**, 1-20.

Ghosh, P., Dahms, N. M. and Kornfeld, S. (2003). Mannose 6-phosphate receptors: new twists in the tale. *Nat. Rev. Mol. Cell Biol.* **4**, 202-212.

Gillingham, A. K. and Munro, S. (2003). Long coiled-coil proteins and membrane traffic. *Biochim. Biophys. Acta* **1641**, 71-85.

Gruenberg, J. and Maxfield, F. R. (1995). Membrane transport in the endocytic pathway. *Curr. Opin. Cell Biol.* **7**, 552-563.

Haglund, K., Sigismund, S., Polo, S., Szymkiewicz, I., Fiore, P. P. D. and Dikic, I. (2003). Multiple monoubiquitination of RTKs is sufficient for their endocytosis and degradation. *Nat. Cell Biol.* **5**, 461-466.

Hopkins, C. R., Gibson, A., Shipman, M. and Miller, K. (1990). Movement of internalized ligand-receptor complexes along a continuous endosomal reticulum. *Nature* **346**, 335-340.

Jing, S., Spencer, T., Miller, K., Hopkins, C. and Trowbridge, I. (1990). Role of the human transferrin receptor cytoplasmic domain in endocytosis: localization of a specific signal sequence for internalization. *J. Cell Biol.* **110**, 283-294.

Katzmann, D. J., Odorizzi, G. and Emr, S. D. (2002). Receptor downregulation and multivesicular-body sorting. *Nat. Rev. Cell Mol. Biol.* **3**, 893-905.

Katzmann, D. J., Stefan, C. J., Babst, M. and Emr, S. D. (2003). Vps27 recruits ESCRT machinery to endosomes during MVB sorting. *J. Cell Biol.* **162**, 413-423.

Komada, M. and Kitamura, N. (1995). Growth factor-induced phosphorylation of Hrs, a novel 115 kDa protein with a structurally conserved putative zinc finger domain. *Mol. Cell. Biol.* **15**, 6213-6221.

Komada, M. and Soriano, P. (1999). Hrs, a FYVE finger protein localized to early endosomes, is implicated in vesicular traffic and required for ventral folding morphogenesis. *Genes Dev.* **13**, 1475-1485.

Lloyd, T. E., Atkinson, R., Wu, M. N., Zhou, Y., Pennetta, G. and Bellen, H. J. (2002). Hrs regulates endosome membrane invagination and tyrosine kinase receptor signaling in *Drosophila*. *Cell* **108**, 261-269.

Martin-Serrano, J., Zang, T. and Bieniasz, P. D. (2001). HIV-1 and Ebola virus encode small peptide motifs that recruit Tsg101 to sites of particle assembly to facilitate egress. *Nat. Med.* **7**, 1313-1319.

Mellman, I. (1996). Endocytosis and molecular sorting. *Ann. Rev. Cell Dev. Biol.* **12**, 575-625.

Nothwehr, S. F., Bryant, N. J. and Stevens, T. H. (1996). The newly identified yeast *GRD* genes are required for retention of late-Golgi membrane proteins. *Mol. Cell. Biol.* **16**, 2700-2707.

Odorizzi, G., Babst, M. and Emr, S. D. (1998). Fab1p PtdIns(3)P 5-kinase function essential for protein sorting in the multivesicular body. *Cell* **95**, 847-858.

Petiot, A., Faure, J., Stenmark, H. and Gruenberg, J. (2003). PI3P signaling regulates receptor sorting but not transport in the endosomal pathway. *J. Cell Biol.* **162**, 971-979.

Piper, R. C., Cooper, A. A., Yang, H. and Stevens, T. H. (1995). *VPS27* controls vacuolar and endocytic traffic through a prevacuolar compartment in *Saccharomyces cerevisiae*. *J. Cell Biol.* **131**, 603-617.

Polo, S., Sigismund, S., Faretta, M., Guidi, M., Capua, M. R., Bossi, G., Chen, H., Camilli, P. D. and Fiore, P. P. D. (2002). A single motif responsible for ubiquitin recognition and monoubiquitination in endocytic proteins. *Nature* **416**, 451-455.

Pornillos, O., Higginson, D. S., Stray, K. M., Fisher, R. D., Garrus, J. E., Payne, M., He, G.-P., Wang, H. E., Morham, S. G. and Sundquist, W. I. (2003). HIV Gag mimics the Tsg101-recruiting activity of the human Hrs protein. *J. Cell Biol.* **162**, 425-434.

Raiborg, C., Gronvold Bache, K., Mehlum, A., Stang, E. and Stenmark, H. (2001). Hrs recruits clathrin to early endosomes. *EMBO J.* **20**, 5008-5021.

Raiborg, C., Bache, K. G., Gillooly, D. J., Madshus, I. H., Stang, E. and Stenmark, H. (2002). Hrs sorts ubiquitinated proteins into clathrin-coated microdomains of early endosomes. *Nat. Cell Biol.* **4**, 394-398.

Raymond, C. K., Howald-Stevenson, I., Vater, C. A. and Stevens, T. H. (1992). Morphological classification of the yeast vacuolar protein sorting mutants: evidence for a prevacuolar compartment in class E *vps* mutants. *Mol. Biol. Cell* **3**, 1389-1402.

Richardson, S. C. W., Winistorfer, S. C., Poupon, V., Luzio, J. P. and Piper, R. C. (2004). Mammalian late vacuole protein sorting orthologues participate in early endosomal fusion and interact with the cytoskeleton. *Mol. Biol. Cell* **15**, 1197-1210.

Rieder, S. E., Banta, L. M., Köhrer, K., McCaffery, J. M. and Emr, S. D. (1996). Multilamellar endosome-like compartment accumulates in the yeast *vps28* vacuolar protein sorting mutant. *Mol. Biol. Cell* **7**, 985-999.

Sachse, M., Urbe, S., Oorschot, V., Strous, G. J. and Klumperman, J. (2002). Bilayered clathrin coats on endosomal vacuoles are involved in protein sorting toward lysosomes. *Mol. Biol. Cell* **13**, 1313-1328.

Sachse, M., Strous, G. J. and Klumperman, J. (2004). ATPase-deficient hVPS4 impairs formation of internal endosomal vesicles and stabilizes bilayered clathrin coats on endosomal vacuoles. *J. Cell Sci.* **117**, 1699-1708.

Seaman, M. N. J. (2004). Cargo-selective endosomal sorting for retrieval to the Golgi requires retromer. *J. Cell Biol.* **165**, 111-122.

Stinchcombe, J. C., Nomoto, H., Cutler, D. F. and Hopkins., C. R. (1995). Anterograde and retrograde traffic between the rough endoplasmic reticulum and the Golgi complex. *J. Cell Biol.* **131**, 1387-1401.

Trowbridge, I. S., Collawn, J. F. and Hopkins, C. R. (1993). Signal-dependent membrane trafficking in the endocytic pathway. *Ann. Rev. Cell Biol.* **9**, 129-161.

Urbe, S., Sachse, M., Row, P. E., Preisinger, C., Barr, F. A., Strous, G., Klumperman, J. and Clague, M. J. (2003). The UIM domain of Hrs couples receptor sorting to vesicle formation. *J. Cell Sci.* **116**, 4169-4179.

van Delft, S., Govers, R., Strous, G. J., Verkleij, A. J. and van Bergen en Henegouwen, P. M. P. (1997). Epidermal growth factor induces ubiquitination of Eps15. *J. Biol. Chem.* **272**, 14013-14016.

van Kerkhof, P., Alves dos Santos, C. M., Sachse, M., Klumperman, J., Bu, G. and Strous, G. J. (2001). Proteasome inhibitors block a late step in lysosomal transport of selected membrane but not soluble proteins. *Mol. Biol. Cell* **12**, 2556-2566.

VerPlank, L., Bouamr, F., LaGrassa, T. J., Agresta, B., Kikonyogo, A., Leis, J. and Carter, C. A. (2001). Tsg101, a homologue of ubiquitin-conjugating (E2) enzymes, binds the L domain in HIV type 1 $Pr55^{Gag}$. *Proc. Natl. Acad. Sci. USA* **98**, 7724-7729.

Zahn, R., Stevenson, B., Schroder-Kohne, S., Zanolari, B., Riezman, H. and Munn, A. (2001). End13p/Vps4p is required for efficient transport from early to late endosomes in *Saccharomyces cerevisiae*. *J. Cell Sci.* **114**, 1935-1947.

Journal of Cell Science